

## WATER DROPLET IMPACT AND SPREADING ON A NARROW GAP

D. Jordan Bouchard and Sanjeev Chandra

Department of Mechanical Engineering  
University of Toronto  
Toronto, Canada

**Abstract**— The impact and spreading of a water droplet on a gap between two parallel plates has been studied experimentally. A deionized water droplet (2.03 mm diameter) impacted the plates at velocities of 0.06, 0.5, 1.0, and 1.5 m/s; the tested gap spacings of the parallel glass plates were 50, 100, and 150  $\mu\text{m}$ . Using a high-speed camera, we simultaneously photographed the drop spreading both above and within the gap. We show that water begins to penetrate the gap immediately after impact. On the largest spacing tested, up to 10% of the initial drop volume can penetrate the gap before the maximum spreading diameter is reached.

*drop spreading; drop impact; parallel plates;*

### I. INTRODUCTION

Many porous surfaces that droplets can interact with – paper, soil, textiles and fabrics – are opaque. This opaqueness makes it difficult to observe how the porous surface interacts with the drop during droplet impact and spreading. In addition, an impacting drop will spread to its maximum diameter in a few milliseconds, well below the temporal resolution of non-destructive scanning techniques.

There remains some uncertainty as to the amount of water that absorbs into a porous media during droplet impact and spreading, and if this volume of water influences the maximum spread of the droplet. Chandra & Avedisian [1] and Lee et al. [2] analyzed photographs of the drop impacting on a porous surface to estimate the volume of water that penetrated a porous material. They conclude that the volume of water is negligibly small for the materials they studied. Roisman et al. [3] find that a porous surface will increase the probability of drop deposition instead of splashing, which they suspect is due to some liquid penetration during impact. Lembach et al. [4] and Yamamoto et al. [5] show that water penetration can occur during droplet impact on their fabricated porous medias. Their medias were fabricated in such a way that allowed them to simultaneously photograph the drop above and below the surface, but the focus of their papers was not on the maximum spread of the droplet.

Thus, there is a need for more experiments that can simultaneously photograph a droplet above and below a surface

during impact in order to understand the role the pore size has on droplet spreading. This is the first experiment in a series designed to investigate how porous media affects how a droplet spreads and penetrates a porous media. Here, we study the influence of a long narrow pore, created by two closely spaced glass plates.

### II. EXPERIMENTAL APPARATUS

Two uncoated N-BK7 borosilicate glass plates (50 mm x 50 mm x 4 mm) (Edmund Optics, Inc; stock# 47-944) were used to create a narrow gap between two parallel surfaces. The gap spacing between the two plates was set by inserting two steel feeler gauges between the plates and then clamping the plates together. Between individual trials, the surfaces of the glass plates were rinsed with deionized water and dried with compressed air. Periodically, the surfaces were cleaned with ethanol and thoroughly rinsed with tap water and then deionized water.

A 10 ml BD syringe was used in a syringe pump to dispense deionized water through a 33-gauge syringe needle (#91033, Hamilton) at a flow rate of 10  $\mu\text{l}/\text{min}$ . A separate test found the average diameter of a drop generated by this method to be 2.03 mm ( $N=50$ , 95%CI). The three gap sizes tested were 50, 100, and 150  $\mu\text{m}$ . The plates were also clamped together with no feeler gauges to get a fourth gap size of approximately 0  $\mu\text{m}$ . Drop impact velocities of 0.06, 0.5, 1.0, and 1.5 m/s were tested by increasing the height at which the drop detached from the syringe needle. Each of the impact velocity-gap spacing pairs was repeated between three and five times. Very good repeatability of the data was achieved.

A high-speed camera (FASTCAM SA5, Photron, USA) equipped with a 105 mm f/2.8 Nikon lens, an extension bellow, and a 55 W LED light (AOS Technologies AG) were used to photograph the droplet spread at a resolution 16.8  $\mu\text{m}/\text{pixel}$ . Photographs were taken at 4000 fps, shutter speed of 1/6000 s. A schematic of the experiment is shown in Figure 1.

Image analysis was performed in MATLAB using an automated script to convert the photographs from the high-speed camera to binary images. The measurement of interest was obtained by counting the number of pixels and multiplying it by the image resolution.

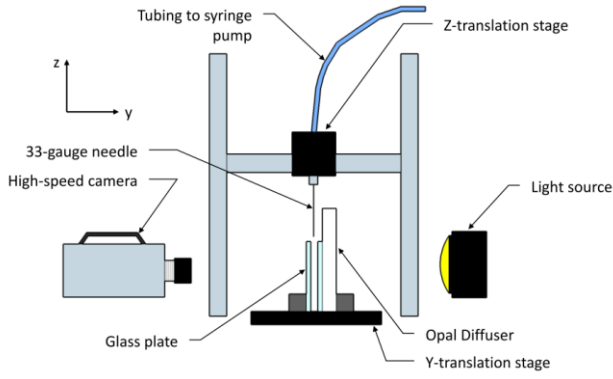


Figure 1. Schematic representation of experiment apparatus

### III. RESULTS AND DISCUSSION

We compare the maximum spreading diameter by first making the spreading diameter and time dimensionless. The droplet spreading diameter is made dimensionless by dividing it by the initial drop diameter,  $\beta = D/D_0$ ; time is made dimensionless by multiplying it by the impact velocity and dividing by the initial drop diameter,  $\tau = Ut/D_0$ , where  $U$  is the impact velocity. Figure 2. shows the dimensionless spreading coefficient,  $\beta$ , plotted against dimensionless time,  $\tau$ . The top, middle, and bottom charts of Figure 2. show the effect of the gap spacing at the constant impact velocities of 0.5, 1.0, and 1.5 m/s, respectively.

At each impact velocity, the maximum spreading diameter increases as the gap spacing decreases. In the 1.5 m/s impact velocity graph of Figure 2. , where this observation is most pronounced, the maximum spreading diameter doubles as the gap spacing is reduced from 150  $\mu\text{m}$  to 0  $\mu\text{m}$ .

Also, the time required to reach the droplet maximum spreading diameter increases as the gap size decreases. At all three impact velocities the drop takes the longest time to spread at zero gap spacing. For example, at an impact velocity of 1.5 m/s, the maximum spreading diameter is reached shortly after  $\tau = 1$  for the 150  $\mu\text{m}$ ; the 100  $\mu\text{m}$  and 50  $\mu\text{m}$  gap sizes take progressively longer, and the longest time of  $\tau = 2.7$  is reached for the at 0  $\mu\text{m}$ .

The maximum spreading diameter and time to maximum spread increase with a decreasing gap size because there is less kinetic energy and liquid available for the drop to spread when a gap is present. We observe that the drop starts to penetrate the gap almost immediately after impact. Photographs of the droplet spreading on the gap at  $\tau = 0.5$  are shown in Figure 3. At every gap spacing and impact velocity a semi-circular profile can be seen developing below the drop before the maximum diameter is reached. With less water remaining in the drop it is unable to spread as far. Time to the maximum spreading diameter is reduced because there is less distance to travel.

It is also interesting to point out in Figure 3. that the shape of the drop is very similar for each impact velocity at each gap

spacing. This is despite there being an increasingly larger volume of water within the gap at successively larger gap spacings. What this means is that immediately after impact the droplet behavior is dominated by inertia, but the influence of the gap spacing becomes apparent before maximum spread is reached. We can see this transition in Figure 2. : the spreading coefficient for each gap size lie on a single curve immediately after impact and then start to diverge before the maximum spreading diameter is reached.

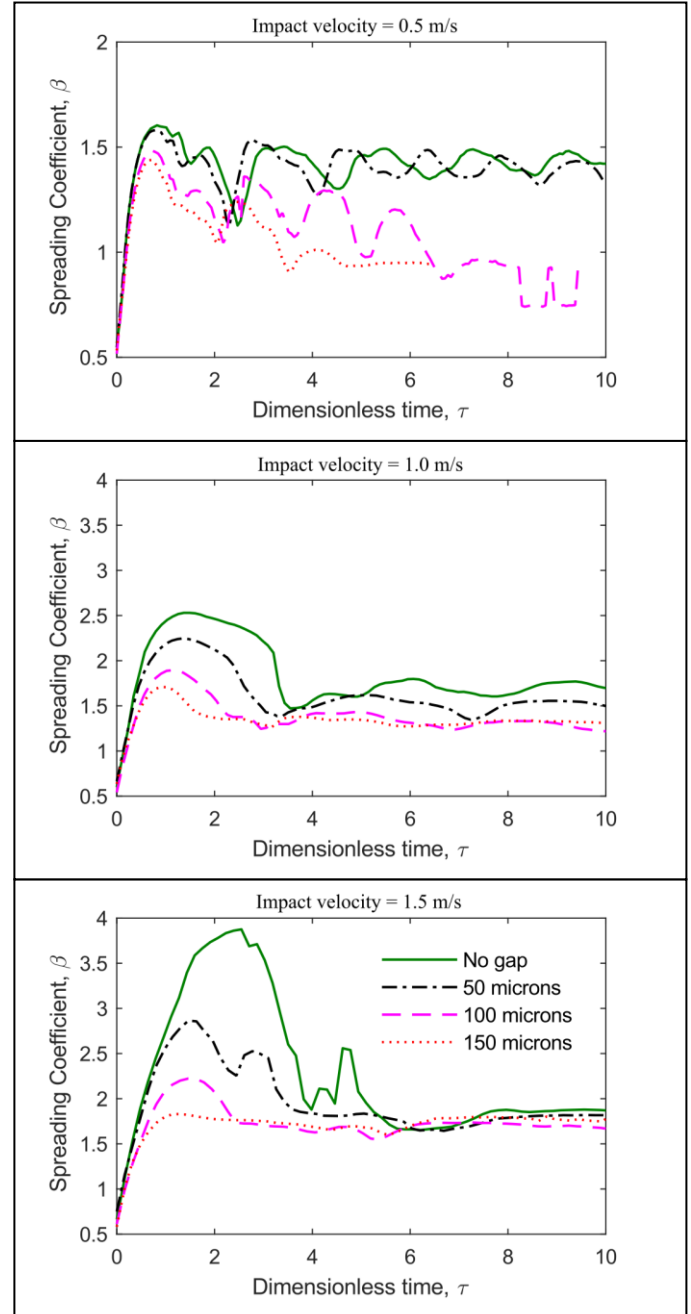


Figure 2. Comparison of dimensionless spreading diameter for impact velocities of 0.5, 1.0, and 1.5 m/s.

Shortly after the drop contacts the glass plates and begins to spread, water wicks into the gap. The width of the profile grows at the same rate as the droplet spreads, but the depth of the profile grows at a different rate. For the 50  $\mu\text{m}$  spacing in Figure 3. , the profile depth reached at  $\tau = 0.5$  decreases slightly as the impact velocity increases. This suggests that the growth rate of the profile width depends on the impact velocity, and that the growth rate of the profile depth depends on the gap spacing, which determines the developed capillary pressure.

Figure 4. shows the fraction of the initial drop volume that penetrates between each plate spacing. The top, middle, and bottom chart are plotted with the gap spacing held constant at 50, 100, and 150  $\mu\text{m}$ , respectively. In the initial stages of the droplet impact and just prior to the maximum spreading diameter being reached, the volume of water in the gap is approximately the same for the 0.5, 1.01 and 1.5 m/s impact velocities. Also shows that the flow rate into the gap is constant shortly after impact, times greater than  $\tau = 0.25$ . Water penetration into the gap during droplet spreading is mostly capillary driven.

The volume of water that can penetrate the gap during droplet spreading is significant for the larger gap spacings. For

the 100 and 150  $\mu\text{m}$  gap spacing, between 5-10% of the drop's initial volume has already entered the gap at  $\tau = 0.5$ . For the 50  $\mu\text{m}$  gap spacing the volume of water that has left the drop by this time is less significant. Despite this large difference in the volume of water that has penetrated the gap, the drops in Figure 3. look very similar for a constant impact velocity. This highlights the difficulty of estimating the volume of water that has penetrated a porous medium during the droplet spreading phase.

#### IV. CONCLUSIONS

When a drop impacts a narrow gap, the maximum spreading diameter will be less than the maximum spreading diameter that could be attained on a solid surface. This is partly due to water penetrating the gap during the spreading phase, so there is less water available within the drop to spread. The volume of water that penetrates the gap is mostly dependent on the width of the gap. A higher fraction of the initial drop volume will be lost to the gap at the time of maximum spread the larger the gap spacing is. The water penetrates mostly due to capillary forces—the impact forces only have a minor influence

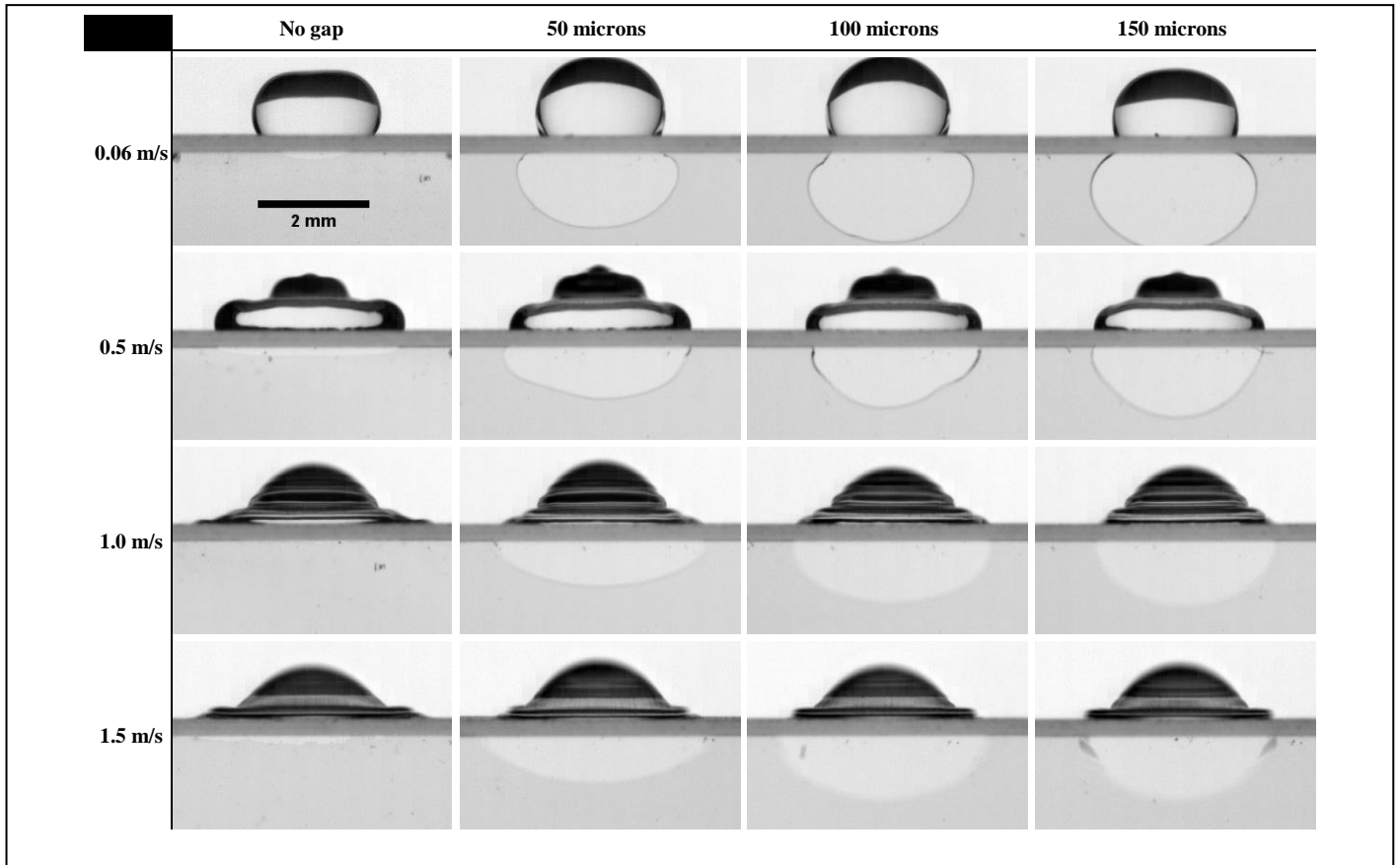


Figure 3. Photographs of a drop impacting on a narrow gap. Rows are a constant impact velocity; columns are a constant gap spacing. Each photograph was taken at dimensionless time,  $\tau = 0.5$ . The images were cropped, scaled, and adjusted for contrast and brightness in ImageJ [6]

## REFERENCES

- [1] S. Chandra and C. T. Avedisian, "Observations of droplet impingement on a ceramic porous surface," *Int. J. Heat Mass Transf.*, vol. 35, no. 10, pp. 2377–2388, 1992.
- [2] J. B. Lee, D. Derome, and J. Carmeliet, "Drop impact on natural porous stones," *J. Colloid Interface Sci.*, vol. 469, pp. 147–156, 2016.
- [3] I. V. Roisman, A. Lembach, and C. Tropea, "Drop splashing induced by target roughness and porosity: The size plays no role," *Adv. Colloid Interface Sci.*, vol. 222, pp. 615–621, 2015.
- [4] A. N. Lembach, I. V. Roisman, and C. Tropea, "Drop impact on porous media," in *DIPSI Workshop 2011 on Drop Impact Phenomena & Spray Investigation*, 2011, no. 1, p. 5.
- [5] K. Yamamoto, H. Takezawa, and S. Ogata, "Droplet impact on textured surfaces composed of commercial stainless razor blades," *Colloids Surfaces A Physicochem. Eng. Asp.*, vol. 506, pp. 363–370, 2016.
- [6] C. A. Schneider, W. S. Rasband, and K. W. Eliceiri, "NIH Image to ImageJ: 25 years of image analysis," *Nat. Methods*, vol. 9, no. 7, pp. 671–675, 2012.

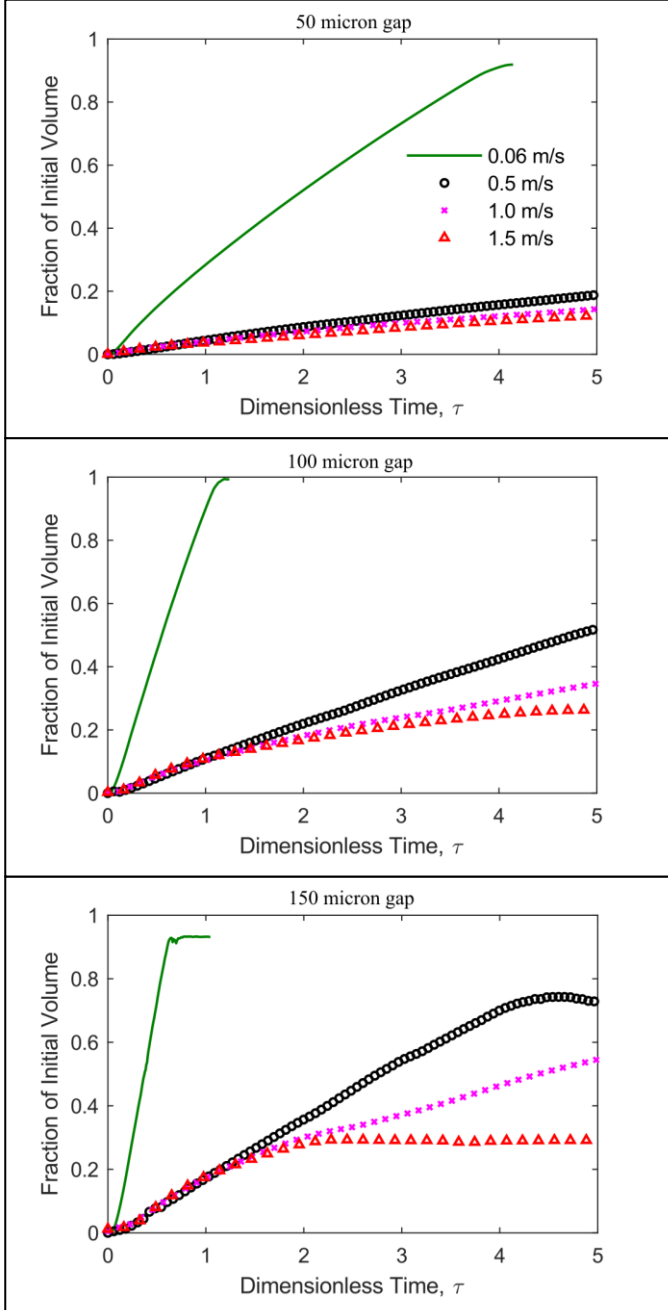


Figure 4. Fraction of initial drop volume that penetrates the plates for gap spacings of 50, 100, and 150  $\mu\text{m}$ .